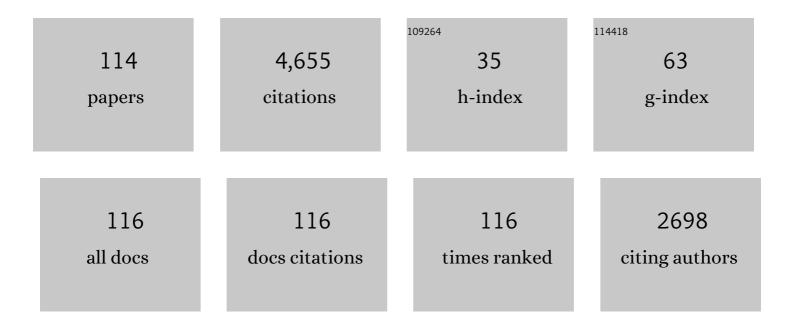
Seok Su Sohn

List of Publications by Year in descending order

Source: https://exaly.com/author-pdf/4551838/publications.pdf Version: 2024-02-01



#	Article	IF	CITATIONS
1	Understanding the physical metallurgy of the CoCrFeMnNi high-entropy alloy: an atomistic simulation study. Npj Computational Materials, 2018, 4, .	3.5	501
2	Ultrastrong Mediumâ€Entropy Singleâ€Phase Alloys Designed via Severe Lattice Distortion. Advanced Materials, 2019, 31, e1807142.	11.1	301
3	Cryogenic strength improvement by utilizing room-temperature deformation twinning in a partially recrystallized VCrMnFeCoNi high-entropy alloy. Nature Communications, 2017, 8, 15719.	5.8	278
4	Effects of Mn and Al contents on cryogenic-temperature tensile and Charpy impact properties in four austenitic high-Mn steels. Acta Materialia, 2015, 100, 39-52.	3.8	194
5	Exceptional phase-transformation strengthening of ferrous medium-entropy alloys at cryogenic temperatures. Acta Materialia, 2018, 161, 388-399.	3.8	174
6	Novel ferrite–austenite duplex lightweight steel with 77% ductility by transformation induced plasticity mechanisms. Acta Materialia, 2014, 78, 181-189.	3.8	140
7	Novel ultra-high-strength (ferrite + austenite) duplex lightweight steels achieved by fine dislocation substructures (Taylor lattices), grain refinement, and partial recrystallization. Acta Materialia, 2015, 96, 301-310.	3.8	135
8	A strong and ductile medium-entropy alloy resists hydrogen embrittlement and corrosion. Nature Communications, 2020, 11, 3081.	5.8	116
9	Novel medium-Mn (austeniteÂ+Âmartensite) duplex hot-rolled steel achieving 1.6ÂGPa strength with 20 % ductility by Mn-segregation-induced TRIP mechanism. Acta Materialia, 2018, 147, 247-260.	3.8	114
10	Novel ultra-high-strength Cu-containing medium-Mn duplex lightweight steels. Acta Materialia, 2017, 135, 215-225.	3.8	100
11	Ultrastrong duplex high-entropy alloy with 2â€ ⁻ GPa cryogenic strength enabled by an accelerated martensitic transformation. Scripta Materialia, 2019, 171, 67-72.	2.6	76
12	FCC to BCC transformation-induced plasticity based on thermodynamic phase stability in novel V10Cr10Fe45CoxNi35â^'x medium-entropy alloys. Scientific Reports, 2019, 9, 2948.	1.6	71
13	Shear band-driven precipitate dispersion for ultrastrong ductile medium-entropy alloys. Nature Communications, 2021, 12, 4703.	5.8	70
14	Effects of martensite-austenite constituent on crack initiation and propagation in inter-critical heat-affected zone of high-strength low-alloy (HSLA) steel. Materials Science & Engineering A: Structural Materials: Properties, Microstructure and Processing, 2018, 715, 332-339.	2.6	67
15	Effects of Mn Addition on Tensile and Charpy Impact Properties in Austenitic Fe-Mn-C-Al-Based Steels for Cryogenic Applications. Metallurgical and Materials Transactions A: Physical Metallurgy and Materials Science, 2014, 45, 5419-5430.	1.1	59
16	Quasi-static and dynamic deformation mechanisms interpreted by microstructural evolution in TWinning Induced Plasticity (TWIP) steel. Materials Science & Engineering A: Structural Materials: Properties, Microstructure and Processing, 2017, 684, 54-63.	2.6	59
17	Cryogenic-temperature fracture toughness analysis of non-equi-atomic V10Cr10Fe45Co20Ni15 high-entropy alloy. Journal of Alloys and Compounds, 2019, 809, 151864.	2.8	57
18	High-rate superplasticity in an equiatomic medium-entropy VCoNi alloy enabled through dynamic recrystallization of a duplex microstructure of ordered phases. Acta Materialia, 2020, 194, 106-117.	3.8	57

#	Article	IF	CITATIONS
19	Microstructural evolution of liquid metal embrittlement in resistance-spot-welded galvanized TWinning-Induced Plasticity (TWIP) steel sheets. Materials Characterization, 2019, 147, 233-241.	1.9	54
20	Effects of Ni and Mn addition on critical crack tip opening displacement (CTOD) of weld-simulated heat-affected zones of three high-strength low-alloy (HSLA) steels. Materials Science & Engineering A: Structural Materials: Properties, Microstructure and Processing, 2017, 697, 55-65.	2.6	52
21	Cu addition effects on TRIP to TWIP transition and tensile property improvement of ultra-high-strength austenitic high-Mn steels. Acta Materialia, 2019, 166, 246-260.	3.8	50
22	Role of brittle sigma phase in cryogenic-temperature-strength improvement of non-equi-atomic Fe-rich VCrMnFeCoNi high entropy alloys. Materials Science & Engineering A: Structural Materials: Properties, Microstructure and Processing, 2018, 724, 403-410.	2.6	49
23	Novel 1.5 GPa-strength with 50%-ductility by transformation-induced plasticity of non-recrystallized austenite in duplex steels. Scientific Reports, 2017, 7, 1255.	1.6	48
24	Reversible dislocation movement, martensitic transformation and nano-twinning during elastic cyclic loading of a metastable high entropy alloy. Acta Materialia, 2020, 185, 474-492.	3.8	48
25	Effects of deformation–induced BCC martensitic transformation and twinning on impact toughness and dynamic tensile response in metastable VCrFeCoNi high–entropy alloy. Journal of Alloys and Compounds, 2019, 785, 1056-1067.	2.8	46
26	Effects of solid solution and grain-boundary segregation of Mo on hydrogen embrittlement in 32MnB5 hot-stamping steels. Acta Materialia, 2021, 207, 116661.	3.8	44
27	Effects of microstructure and yield ratio on strain hardening and Bauschinger effect in two API X80 linepipe steels. Materials Science & Engineering A: Structural Materials: Properties, Microstructure and Processing, 2012, 551, 192-199.	2.6	43
28	Effects of Nb and Mo alloying on resistance to hydrogen embrittlement in 1.9ÂGPa-grade hot-stamping steels. Materials Science & Engineering A: Structural Materials: Properties, Microstructure and Processing, 2020, 789, 139656.	2.6	43
29	Effect of Austenite Stability on Microstructural Evolution and Tensile Properties in Intercritically Annealed Medium-Mn Lightweight Steels. Metallurgical and Materials Transactions A: Physical Metallurgy and Materials Science, 2016, 47, 2674-2685.	1.1	41
30	Effects of transformation-induced plasticity (TRIP) on tensile property improvement of Fe45Co30Cr10V10Ni5-xMnx high-entropy alloys. Materials Science & Engineering A: Structural Materials: Properties, Microstructure and Processing, 2020, 772, 138809.	2.6	41
31	Analysis of damage-tolerance of TRIP-assisted V10Cr10Fe45Co30Ni5 high-entropy alloy at room and cryogenic temperatures. Journal of Alloys and Compounds, 2020, 844, 156090.	2.8	41
32	Interpretation of cryogenic-temperature Charpy fracture initiation and propagation energies by microstructural evolution occurring during dynamic compressive test of austenitic Fe–(0.4,1.0)C–18Mn steels. Materials Science & Engineering A: Structural Materials: Properties, Microstructure and Processing, 2015, 641, 340-347.	2.6	40
33	Dynamic compressive deformation behavior of SiC-particulate-reinforced A356 Al alloy matrix composites fabricated by liquid pressing process. Materials Science & Engineering A: Structural Materials: Properties, Microstructure and Processing, 2017, 680, 368-377.	2.6	40
34	Effects of Cu addition on resistance to hydrogen embrittlement in 1ÂGPa-grade duplex lightweight steels. Acta Materialia, 2020, 196, 370-383.	3.8	39
35	Key factors of stretch-flangeability of sheet materials. Journal of Materials Science, 2017, 52, 7808-7823.	1.7	38
36	Ultra-strong and strain-hardenable ultrafine-grained medium-entropy alloy via enhanced grain-boundary strengthening. Materials Research Letters, 2021, 9, 315-321.	4.1	38

#	Article	IF	CITATIONS
37	Dramatic improvement of strain hardening and ductility to 95% in highly-deformable high-strength duplex lightweight steels. Scientific Reports, 2017, 7, 1927.	1.6	37
38	Effects of annealing temperature on microstructures and tensile properties of a single FCC phase CoCuMnNi high-entropy alloy. Journal of Alloys and Compounds, 2020, 812, 152111.	2.8	37
39	Effects of cryogenic temperature on tensile and impact properties in a medium-entropy VCoNi alloy. Journal of Materials Science and Technology, 2021, 90, 159-167.	5.6	36
40	Dynamic tension–compression asymmetry of martensitic transformation in austenitic Fe–(0.4,) Tj ETQq0 0	0 rgBT /O	verlgck 10 Tf 5
41	Understanding of adiabatic shear band evolution during high-strain-rate deformation in high-strength armor steel. Journal of Alloys and Compounds, 2020, 845, 155540.	2.8	34
42	Effects of Ni and Cu addition on cryogenic-temperature tensile and Charpy impact properties in austenitic 22Mn-0.45C–1Al steels. Journal of Alloys and Compounds, 2020, 815, 152407.	2.8	31
43	Thermodynamic analysis of the effect of C, Mn and Al on microstructural evolution of lightweight steels. Scripta Materialia, 2013, 68, 339-342.	2.6	30
44	Effect of solid-solution strengthening on deformation mechanisms and strain hardening in medium-entropy V1-Cr CoNi alloys. Journal of Materials Science and Technology, 2022, 108, 270-280.	5.6	30
45	Effects of finish rolling temperature on inverse fracture occurring during drop weight tear test of API X80 pipeline steels. Materials Science & Engineering A: Structural Materials: Properties, Microstructure and Processing, 2012, 541, 181-189.	2.6	29
46	Microstructural analysis of cracking phenomenon occurring during cold rolling of (0.1~0.7)C-3Mn-5Al lightweight steels. Metals and Materials International, 2015, 21, 43-53.	1.8	29
47	Effects of Ti alloying on resistance to hydrogen embrittlement in (Nb+Mo)-alloyed ultra-high-strength hot-stamping steels. Materials Science & Engineering A: Structural Materials: Properties, Microstructure and Processing, 2020, 791, 139763.	2.6	29
48	A thermodynamic description of the Co-Cr-Fe-Ni-V system for high-entropy alloy design. Calphad: Computer Coupling of Phase Diagrams and Thermochemistry, 2019, 66, 101624.	0.7	28
49	Effects of solute segregation on tensile properties and serration behavior in ultra-high-strength high-Mn TRIP steels. Materials Science & Engineering A: Structural Materials: Properties, Microstructure and Processing, 2019, 740-741, 16-27.	2.6	28
50	Effects of Cr addition on Charpy impact energy in austenitic 0.45C-24Mn-(0,3,6)Cr steels. Journal of Materials Science and Technology, 2020, 50, 21-30.	5.6	28
51	Tensile property improvement of TWIP-cored three-layer steel sheets fabricated by hot-roll-bonding with low-carbon steel or interstitial-free steel. Scientific Reports, 2017, 7, 40231.	1.6	27
52	Interpretation of quasi-static and dynamic tensile behavior by digital image correlation technique in TWinning Induced Plasticity (TWIP) and low-carbon steel sheets. Materials Science & Engineering A: Structural Materials: Properties, Microstructure and Processing, 2017, 693, 170-177.	2.6	27
53	A Thermodynamic Modelling of the Stability of Sigma Phase in the Cr-Fe-Ni-V High-Entropy Alloy System. Journal of Phase Equilibria and Diffusion, 2018, 39, 694-701.	0.5	27
54	Effects of coiling temperature and pipe-forming strain on yield strength variation after ERW pipe forming of API X70 and X80 linepipe steels. Materials Science & Engineering A: Structural Materials: Properties, Microstructure and Processing, 2017, 682, 304-311.	2.6	25

4

#	Article	IF	CITATIONS
55	Effects of Al-Si coating structures on bendability and resistance to hydrogen embrittlement in 1.5-GPa-grade hot-press-forming steel. Acta Materialia, 2022, 225, 117561.	3.8	25
56	Effects of microstructure and pre-strain on Bauschinger effect in API X70 and X80 linepipe steels. Metals and Materials International, 2013, 19, 423-431.	1.8	24
57	Microstructural Developments and Tensile Properties of Lean Fe-Mn-Al-C Lightweight Steels. Jom, 2014, 66, 1857-1867.	0.9	24
58	Ultra-high strength and excellent ductility in multi-layer steel sheet of austenitic hadfield and martensitic hot-press-forming steels. Materials Science & Engineering A: Structural Materials: Properties, Microstructure and Processing, 2019, 759, 320-328.	2.6	24
59	Effects of Al addition on tensile properties of partially recrystallized austenitic TRIP/TWIP steels. Materials Science & Engineering A: Structural Materials: Properties, Microstructure and Processing, 2021, 806, 140823.	2.6	24
60	Tensile properties of cold-rolled TWIP-cored three-layer steel sheets. Materials Science & Engineering A: Structural Materials: Properties, Microstructure and Processing, 2017, 686, 160-167.	2.6	23
61	Effects of untransformed ferrite on Charpy impact toughness in 1.8-GPa-grade hot-press-forming steel sheets. Materials Science & Engineering A: Structural Materials: Properties, Microstructure and Processing, 2017, 707, 65-72.	2.6	23
62	Effect of tempering conditions on adiabatic shear banding during dynamic compression and ballistic impact tests of ultra-high-strength armor steel. Materials Science & Engineering A: Structural Materials: Properties, Microstructure and Processing, 2020, 792, 139818.	2.6	23
63	Effects of microstructure and pipe forming strain on yield strength before and after spiral pipe forming of API X70 and X80 linepipe steel sheets. Materials Science & Engineering A: Structural Materials: Properties, Microstructure and Processing, 2013, 573, 18-26.	2.6	22
64	Effects of Oxides on Tensile and Charpy Impact Properties and Fracture Toughness in Heat Affected Zones of Oxide-Containing API X80 Linepipe Steels. Metallurgical and Materials Transactions A: Physical Metallurgy and Materials Science, 2014, 45, 3036-3050.	1.1	22
65	Austenite reversion through subzero transformation and tempering of a boron-doped strong and ductile medium-Mn lightweight steel. Materials Science & Engineering A: Structural Materials: Properties, Microstructure and Processing, 2021, 802, 140619.	2.6	22
66	Achievement of high yield strength and strain hardening rate by forming fine ferrite and dislocation substructures in duplex lightweight steel. Materials Science & Engineering A: Structural Materials: Properties, Microstructure and Processing, 2017, 704, 287-291.	2.6	21
67	Improvement of tensile properties in (austenite+ferrite+l̂º-carbide) triplex hot-rolled lightweight steels. Materials Science & Engineering A: Structural Materials: Properties, Microstructure and Processing, 2018, 730, 177-186.	2.6	21
68	Effects of Annealing Treatment Prior to Cold Rolling on the Edge Cracking Phenomenon of Ferritic Lightweight Steel. Metallurgical and Materials Transactions A: Physical Metallurgy and Materials Science, 2014, 45, 3844-3856.	1.1	20
69	Effects of deformation-induced martensitic transformation on cryogenic fracture toughness for metastable Si8V2Fe45Cr10Mn5Co30 high-entropy alloy. Acta Materialia, 2022, 225, 117568.	3.8	20
70	Effects of Annealing Treatment Prior to Cold Rolling on Delayed Fracture Properties in Ferrite-Austenite Duplex Lightweight Steels. Metallurgical and Materials Transactions A: Physical Metallurgy and Materials Science, 2016, 47, 706-717.	1.1	18
71	Characterization of twin-like structure in a ferrite-based lightweight steel. Metals and Materials International, 2016, 22, 810-816.	1.8	17
72	Role of retained austenite on adiabatic shear band formation during high strain rate loading in high-strength bainitic steels. Materials Science & Engineering A: Structural Materials: Properties, Microstructure and Processing, 2020, 778, 139118.	2.6	17

#	Article	IF	CITATIONS
73	Effects of local-brittle-zone (LBZ) microstructures on crack initiation and propagation in three Mo-added high-strength low-alloy (HSLA) steels. Materials Science & Engineering A: Structural Materials: Properties, Microstructure and Processing, 2019, 760, 125-133.	2.6	16
74	Effect of Mn Addition on Microstructural Modification and Cracking Behavior of Ferritic Light-Weight Steels. Metallurgical and Materials Transactions A: Physical Metallurgy and Materials Science, 2014, 45, 5469-5485.	1.1	15
75	Dynamic tensile behavior of twinning-induced plasticity/low-carbon (TWIP/LC) steel clad sheets bonded by hot rolling. Materials Science & Engineering A: Structural Materials: Properties, Microstructure and Processing, 2017, 700, 387-396.	2.6	15
76	Correlation of dynamic compressive properties, adiabatic shear banding, and ballistic performance of high-strength 2139 and 7056 aluminum alloys. Materials Science & Engineering A: Structural Materials: Properties, Microstructure and Processing, 2021, 804, 140757.	2.6	15
77	The microstructure evolution and room temperature deformation behavior of ferrite-based lightweight steel. Materials Science & Engineering A: Structural Materials: Properties, Microstructure and Processing, 2016, 665, 10-16.	2.6	14
78	Body-centered-cubic martensite and the role on room-temperature tensile properties in Si-added SiVCrMnFeCo high-entropy alloys. Journal of Materials Science and Technology, 2021, 76, 222-230.	5.6	14
79	Effects of Nb or (NbÂ+ÂMo) alloying on Charpy impact, bending, and delayed fracture properties in 1.9-GPa-grade press hardening steels. Materials Characterization, 2021, 176, 111133.	1.9	13
80	On the fatigue and dwell-fatigue behavior of a low-density steel and the correlated microstructure origin of damage mechanism. Journal of Materials Research and Technology, 2021, 15, 6136-6154.	2.6	13
81	Novel twin-roll-cast Ti/Al clad sheets with excellent tensile properties. Scientific Reports, 2017, 7, 8110.	1.6	12
82	Interpretation of dynamic tensile behavior by austenite stability in ferrite-austenite duplex lightweight steels. Scientific Reports, 2017, 7, 15726.	1.6	12
83	Exceptional combination of ultra-high strength and excellent ductility by inevitably generated Mn-segregation in austenitic steel. Materials Science & Engineering A: Structural Materials: Properties, Microstructure and Processing, 2018, 737, 69-76.	2.6	12
84	Enhancement of ballistic performance enabled by transformation-induced plasticity in high-strength bainitic steel. Journal of Materials Science and Technology, 2021, 84, 219-229.	5.6	12
85	Computational design of V-CoCrFeMnNi high-entropy alloys: An atomistic simulation study. Calphad: Computer Coupling of Phase Diagrams and Thermochemistry, 2021, 74, 102317.	0.7	12
86	Effects of Cr and Nb addition on high-temperature tensile properties in austenitic cast steels used for turbo-charger application. Materials Science & Engineering A: Structural Materials: Properties, Microstructure and Processing, 2016, 677, 316-324.	2.6	11
87	Study of Bauschinger effect of acicular ferrite and polygonal ferrite through ex-situ interrupted bending tests in API X80 linepipe steels. Scientific Reports, 2018, 8, 15598.	1.6	11
88	Analysis and estimation of the yield strength of API X70 and X80 linepipe steels by double-cycle simulation tests. Metals and Materials International, 2013, 19, 377-388.	1.8	10
89	Adiabatic shear banding and cracking phenomena occurring during cold-forging simulation tests of plain carbon steel wire rods by using a split Hopkinson's pressure bar. Metals and Materials International, 2015, 21, 991-999.	1.8	10
90	Three-Ply Al/Mg/Al Clad Sheets Fabricated by Twin-Roll Casting and Post-treatments (Homogenization,) Tj ETQ	q0 0 0 rgBT 1.1	/Overlock 10

Materials Science, 2017, 48, 57-62.

#	Article	IF	CITATIONS
91	Suppression of adiabatic shear band formation by martensitic transformation of retained austenite during split Hopkinson pressure bar test for a high-strength bainitic steel. Materials Science & Engineering A: Structural Materials: Properties, Microstructure and Processing, 2021, 814, 141127.	2.6	10
92	Effects of Cu addition on formability and surface delamination phenomenon in high-strength high-Mn steels. Journal of Materials Science and Technology, 2020, 43, 44-51.	5.6	9
93	Overcoming strength-ductility trade-off via subzero martensitic transformation in medium-Mn lightweight steel. Scripta Materialia, 2022, 210, 114477.	2.6	9
94	Effect of Strain-Induced Age Hardening on Yield Strength Improvement in Ferrite-Austenite Duplex Lightweight Steels. Metallurgical and Materials Transactions A: Physical Metallurgy and Materials Science, 2016, 47, 5372-5382.	1.1	8
95	Dynamic strain aging and twin formation during warm deformation of a novel medium-entropy lightweight steel. Journal of Materials Research and Technology, 2022, 17, 1628-1641.	2.6	8
96	Ultrasonic nanocrystal surface modification for strength improvement and suppression of hydrogen permeation in multi-layered steel. Journal of Alloys and Compounds, 2021, 885, 160975.	2.8	7
97	Effects of granular bainite and polygonal ferrite on yield point phenomenon in API X65 line-pipe steels. Materials Science & Engineering A: Structural Materials: Properties, Microstructure and Processing, 2022, 840, 143006.	2.6	7
98	Dynamic tensile deformation behavior of Zr-based amorphous alloy matrix composites reinforced with tungsten or tantalum fibers. Metals and Materials International, 2016, 22, 707-713.	1.8	6
99	Simulation of Pipe-Manufacturing Processes Using Sheet Bending-Flattening. Experimental Mechanics, 2018, 58, 909-918.	1.1	6
100	Analysis and estimation of yield strength of API X80 linepipe steel pipe by low-cycle fatigue tests. Metals and Materials International, 2012, 18, 597-606.	1.8	5
101	Effects of temperature and loading rate on phase stability and deformation mechanism in metastable V10Cr10Co30FexNi50-x high entropy alloys. Materials Science & Engineering A: Structural Materials: Properties, Microstructure and Processing, 2021, 804, 140766.	2.6	5
102	Excellent strength-ductility combination of multi-layered sheets composed of high-strength V10Cr10Fe50Co30 high entropy alloy and 304 austenitic stainless steel. Materials Science & Engineering A: Structural Materials: Properties, Microstructure and Processing, 2021, 823, 141727.	2.6	5
103	Effects of Mn Segregations on Intergranular Fracture in a Mediumâ€Mn Lowâ€Density Steel. Steel Research International, 2023, 94, .	1.0	5
104	In Situ fracture observation and fracture toughness analysis of pearlitic graphite cast irons with different nodularity. Metals and Materials International, 2013, 19, 673-682.	1.8	4
105	Interpretation of high-temperature tensile properties by thermodynamically calculated equilibrium phase diagrams of heat-resistant austenitic cast steels. Metals and Materials International, 2017, 23, 43-53.	1.8	4
106	Strength–ductility enhancement in multi-layered sheet with high-entropy alloy and high-Mn twinning-induced plasticity steel. Materials Science & Engineering A: Structural Materials: Properties, Microstructure and Processing, 2021, 822, 141670.	2.6	4
107	Effects of granular bainite and polygonal ferrite on yield strength anisotropy in API X65 linepipe steel. Materials Science & Engineering A: Structural Materials: Properties, Microstructure and Processing, 2022, 843, 143151.	2.6	4
108	Effects of Cr Reduction on High-Temperature Strength of High-Ni Austenitic Cast Steels Used for High-Performance Turbo-chargers. Metallurgical and Materials Transactions A: Physical Metallurgy and Materials Science, 2018, 49, 4604-4614.	1.1	3

#	Article	IF	CITATIONS
109	Effects of V or Cu Addition on High-Temperature Tensile Properties of High-Ni-Containing Austenitic Cast Steels Used for High-Performance Turbo-Charger Housings. Metals and Materials International, 2019, 25, 285-294.	1.8	3
110	Effects of finish rolling temperature and yield ratio on variations in yield strength after pipe-forming of API-X65 line-pipe steels. Scientific Reports, 2020, 10, 14742.	1.6	3
111	Strong resistance to hydrogen embrittlement via surface shielding in multi-layered austenite/martensite steel sheets. Materials Science & Engineering A: Structural Materials: Properties, Microstructure and Processing, 2021, 800, 140319.	2.6	3
112	Interpretation of surficial shear crack propagation mechanisms in bending for Zn or AlSi coated hot press forming steels. Scientific Reports, 2021, 11, 11428.	1.6	2
113	Effect of Intercritical Heat Treatment on J-R Fracture Resistance of SA508 Gr.1A Low-Alloy Steels. Metals and Materials International, 0, , .	1.8	2
114	Enhancement of ballistic performance enabled by boron-doping in subzero-treated (ferrite+austenite+martensite) triplex lightweight steel. Materials Characterization, 2022, 190, 112021.	1.9	2